

Fluid Simulation on Subcycle Wave Generation in Relativistic Laser-Plasma Interactions

HOJO Hitoshi, AKIMOTO Kazuhiro¹ and WATANABE Tsuguhiro²

Plasma Research Center, University of Tsukuba, Tsukuba 305-8577, Japan

¹*School of Science and Engineering, Teikyo University, Utsunomiya 320-8551, Japan*

²*National Institute for Fusion Science, Toki 509-5292, Japan*

(Received: 12 December 2003 / Accepted: 20 April 2004)

Abstract

The generation of subcycle electromagnetic waves with linear polarization in relativistic laser-plasma interactions is demonstrated in one-dimensional fluid simulations for a cold plasma. It is shown that the width (FWHM) of the generated ultrashort pulse is less than one carrier wavelength, that is, the generated ultrashort pulse is a subcycle electromagnetic wave with finite propagation speed. The associated wake field following just behind the generated subcycle electromagnetic wave is demonstrated. The stationary solutions of subcycle waves with circular polarization are also obtained.

Keywords:

computer simulation, subcycle wave, ultraintense field, laser-plasma interaction, relativistic plasma

1. Introduction

The formation of solitary electromagnetic waves in ultraintense relativistic laser-plasma interactions has been recently receiving growing attention, and many theoretical [1-5] and numerical [6-8] works have been reported. The simulation studies are based on PIC particle codes. In the one-dimensional stationary propagation, Eriskepov *et al.* [1] have found an exact solitary-wave solution of relativistic electromagnetic wave, which is standing called as “post soliton [8]”. Hojo and Akimoto [2] have also shown numerically that the same equation describing the above solution has a solitary wave solution moving with finite velocity. More recently, solitary-wave solutions of relativistic electromagnetic wave have been reported for magnetized plasmas [3], electron-movable ion plasmas [4], and electron-positron plasmas [5].

The aim of this paper is to show the generation of nonlinear subcycle electromagnetic waves in one-dimensional fluid simulation on relativistic laser-plasma interactions. The use of the fluid code is that more accurate computations with less noises would be expected in wave propagation analysis as compared with particle simulations. In the following section, we describe the basic equations used for simulations, and briefly describe stationary subcycle solutions with circular polarization in section 3, and show the simulation results for the subcycle wave generation in section 4.

2. Basic equations for simulations

The starting point is Maxwell equations and fluid equations of the electron and ion for a cold plasma in one dimension given by

$$\frac{\partial}{\partial t} \mathbf{B} = -\nabla \times \mathbf{E}, \quad (1)$$

$$\frac{\partial}{\partial t} \mathbf{E} = \nabla \times \mathbf{B} + n \frac{\mathbf{p}}{\gamma} - N \mathbf{V}, \quad (2)$$

$$\left(\frac{\partial}{\partial t} + \frac{p_z}{\gamma} \frac{\partial}{\partial z} \right) \mathbf{p} = -\mathbf{E} - \frac{\mathbf{p}}{\gamma} \times \mathbf{B}, \quad (3)$$

$$n = N - \frac{\partial}{\partial z} E_z, \quad (4)$$

$$\frac{\partial}{\partial t} N + \frac{\partial}{\partial z} (N V_z) = 0, \quad (5)$$

$$\frac{\partial}{\partial t} \mathbf{V} = \frac{m}{M} \mathbf{E}, \quad (6)$$

where $\gamma = (1 + p^2)^{1/2}$ and the mass ratio $m/M = 1/1836$ is assumed. Here, the following normalization was used: $\omega_{p0} t \rightarrow t$, $\omega_{p0} z/c \rightarrow z$, $e\mathbf{E}/\omega_{p0} mc \rightarrow \mathbf{E}$, $e\mathbf{B}/\omega_{p0} m \rightarrow \mathbf{B}$, $\mathbf{P}/mc \rightarrow \mathbf{P}$, $\mathbf{V}/c \rightarrow \mathbf{V}$, $n/n_0 \rightarrow n$, $N/n_0 \rightarrow N$, where $\omega_{p0} = (e^2 n_0 / \epsilon_0 m)^{1/2}$ and

n_0 is a constant density. Here, the equation of motion for the ion is linearized, although that for the electron is relativistic. This approximation for the ion is valid for the present simulation parameters. In the simulation, the electron density n is obtained from the Poisson equation, on the other hand, the ion density N is obtained from the continuity equation. The numerical scheme is that the spatial derivative is replaced by the central difference, the resultant ordinary differential equations are solved by the Runge-Kutta method of the third order. We note that a dissipative term $-v(\partial^2/\partial z^2)\mathbf{p}$ is introduced to suppress short-wavelength oscillations due to numerical errors, and that the qualitative feature on the subcycle wave generation does not depend on the value of v , however, the onset time of the generation and the amplitude of excited wakefield following after the excited subcycle wave strongly depend on v .

3. Stationary subcycle wave

In this section, we consider stationary solutions of subcycle electromagnetic waves with circular polarization in the case of immobile ions. If we introduce vector and scalar potentials, \mathbf{a} and ϕ , defined respectively by

$$\mathbf{E} = -\nabla\phi - \frac{\partial}{\partial t}\mathbf{a}, \quad \mathbf{B} = \nabla \times \mathbf{a} \quad (7)$$

with $\nabla \cdot \mathbf{a} = 0$, and considering a circularly polarized mode with $a_x + ia_y = a(\xi)\exp\{i\omega[(1-V^2)t - V\xi]\}$, we can obtain [1]

$$\frac{d^2}{d\xi^2} a = \frac{1}{1-V^2} \frac{a}{\gamma-b} - \omega^2 a, \quad (8)$$

$$\frac{d^2}{d\xi^2} \phi = \frac{b}{\gamma-b}, \quad (9)$$

$$\gamma = \sqrt{1+a^2+V^2b^2} = 1 + \phi + V^2b, \quad (10)$$

where $\xi = z - Vt$ and V is the propagating speed normalized by c . We note that ω being normalized by ω_{pe} comes up to 1 when $a \rightarrow 0$, and the nonlinear frequency shift is proportional to $1 - \omega$.

For $V = 0$, Eqs. (8)-(10) are reduced to

$$\frac{d^2}{d\xi^2} a = a \left[\gamma - \omega^2 \gamma^2 + \frac{1}{\gamma^2} \left(\frac{da}{d\xi} \right)^2 \right] \quad (11)$$

with $\gamma = (1+a^2)^{1/2}$ [2]. Equation (11) does not reduce to the stationary form of the nonlinear Schrödinger equation with cubic nonlinearity even to the third order in a due to the existence of $(da/d\xi)^2$. However, it can be shown that its exact solitary-wave solution [1] is reduced to the waveform of sech (ξ) in the lowest order of a .

We now solve Eqs. (8)-(10) numerically with the boundary condition in which a and ϕ vanish to zero at $|\xi| \rightarrow \infty$. In Fig.1, we show the solitary-wave solutions for $V =$

0.1 and $\omega = 0.97799$ (a), 0.79 (b). The solitary-wave amplitude increases and the pulse-width decreases for the larger nonlinear frequency shift (i.e., for the smaller ω). We see that the profiles of ϕ and n become acute at $\xi \approx 0$ for a large-amplitude wave. In Fig. 2, we show the maximum amplitudes of a and ϕ , and the minimum value of n as a function of ω .

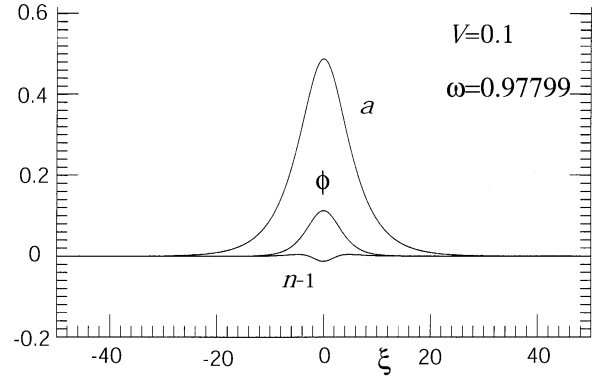


Fig. 1 (a) Subcycle wave for $V = 0.1$ and $\omega = 0.97799$.

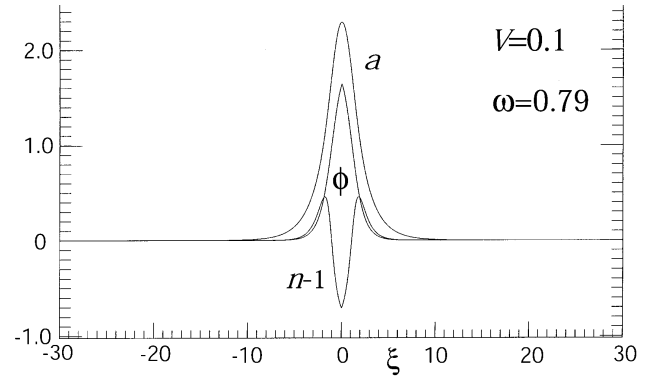


Fig. 1 (b) Subcycle wave for $V = 0.1$ and $\omega = 0.79$.

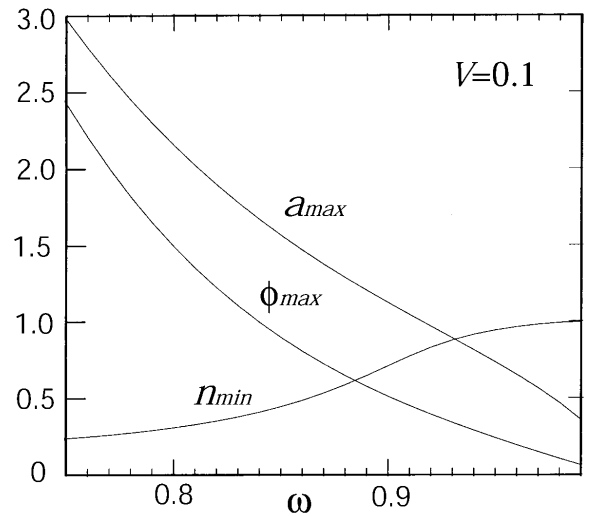


Fig. 2 The wave amplitudes a_{max} , ϕ_{max} and n_{min} vs. ω for $V = 0.1$.

4. Simulation results

In this section, we show the results from fluid simulations based on the equations discussed in section 2. The initial laser pulse is excited at the left-hand side ($z = 0$) in the simulation area and the boundary condition at the right-hand side is the out-going wave condition. The initial density profile at $t = 0$ is given by

$$n(z) = N(z) = \{1 + \tanh[(z - 300)/10]\}/2. \quad (12)$$

That is, a laser pulse is generated in the vacuum region and is launched into a plasma region. The initial laser pulse with linear polarization is assumed to have the waveform of Gaussian pulse given by

$$E_x(t) = E_0 \exp[-(t - t_0)^2 / D^2] \sin(\omega t). \quad (13)$$

We show the simulation result on subcycle wave generation in Fig. 3, where $E_0 = 0.8$, $\omega = 2$, $D = 10$, $t_0 = 20$, $\nu = 2.5 \times 10^{-4}$, $\Delta z = 0.05$, and $\Delta t = 0.0025$ (in the normalized values). We see that, for the launched laser pulse into a plasma, the steepening of the wave form takes place, and then that the laser pulse is separated into two parts of a newly-generated ultrashort pulse with large amplitude and the small-amplitude longer pulse in a plasma. The FWHM of the newly-generated ultrashort pulse in E_x is about 0.8λ at $t = 1400$, λ being the carrier wavenumber of a laser pulse. Therefore, the generated pulse is a subcycle electromagnetic wave. On the other hand, the small-amplitude longer pulse is seemed to be expanding with time due to the dispersion effect in a plasma. The speed of the generated subcycle wave is $V/c = 0.57$ at $t = 1200$, and is gradually decreasing with time, but tends to be saturated. The gradual slowdown of the speed is supposed to be due to the slow decorrelation with the small-amplitude longer pulse. The feature of this generated subcycle wave is different from that obtained in the particle simulations [1,6-8], where the generated subcycle wave is almost standing.

We show the wake field E_z associated with E_x at $t = 1200$ in Fig. 4. We see that the wake field follows just behind the newly-generated subcycle wave. The amplitude of the wake field is about $E_z \approx 0.1$. The wake field is an electrostatic plasma wave and it is often used for plasma-particle acceleration such as the laser wake field acceleration. The close-up figure of E_x and E_z at $t = 1200$ is shown in Fig. 5, where the value of E_z is multiplied by ten times. We suppose that the complex behavior of the wakefield depends on the phase relation between the wakefield (E_z) and the large-amplitude part of an incident laser pulse (E_x), which is developing into a subcycle pulse. However, this problem is considered to be a future research subject.

Finally, as the intense subcycle electromagnetic wave is shown to accelerate charged particles very efficiently [9], we believe in that the present study on the generation of subcycle electromagnetic waves is useful in charged particle acceleration researches.

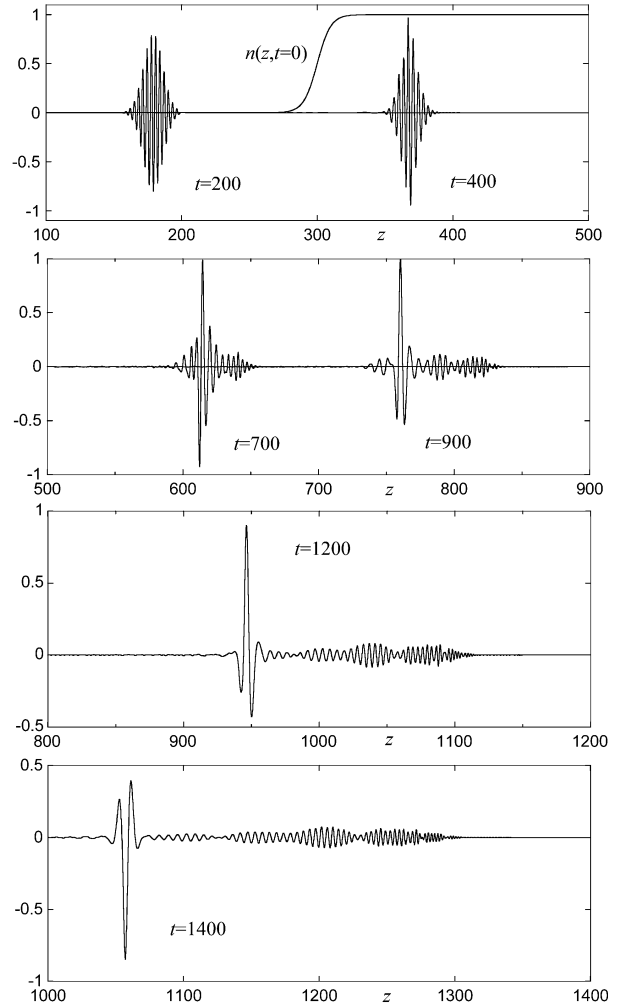


Fig. 3 The temporal behavior of laser pulse E_x .

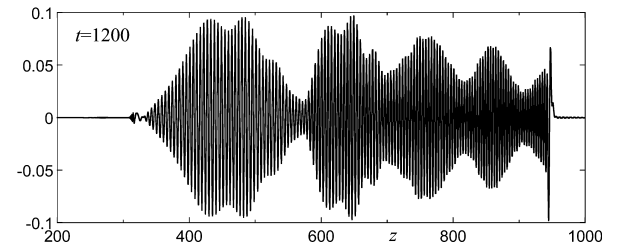


Fig. 4 The profile of wake field E_z at $t = 1200$.

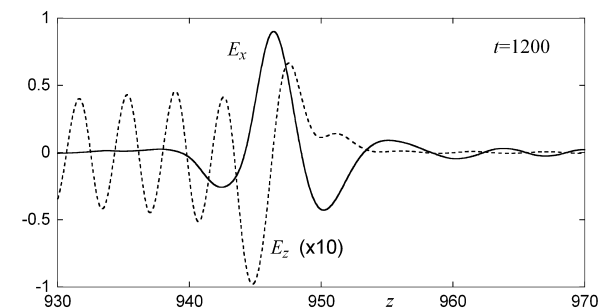


Fig. 5 The close-up of E_x and E_z at $t = 1200$.

References

- [1] T. Zh. Esirkepov *et al.*, JETP Lett. **68**, 36 (1998).
- [2] H. Hojo and K. Akimoto, *Proc. Int. Cong. Plasma Phys.* (Quebec, 2000), p.556.
- [3] D. Farina *et al.*, Phys. Rev. **E 62**, 4146 (2000).
- [4] D. Farina and S. Bulanov, Phys. Rev. Lett. **86**, 5289 (2001).
- [5] D. Farina and S. Bulanov, Phys. Rev. **E 64**, 066401 (2001).
- [6] S. Bulanov *et al.*, Phys. Rev. Lett. **82**, 3440 (1999).
- [7] Y. Sentoku *et al.*, Phys. Rev. Lett. **83**, 3434 (1999).
- [8] N. Naumova *et al.*, Phys. Rev. Lett. **87**, 185004 (2001).
- [9] B. Rau *et al.*, Phys. Rev. Lett. **78**, 3310 (1997).